



**Fermi National Accelerator Laboratory**

**FERMILAB-Conf-97/167-E**  
**CDF**

## **Jet Physics at CDF**

Philip Mèlèse  
For the CDF Collaboration

*Fermi National Accelerator Laboratory  
P.O. Box 500, Batavia, Illinois 60510*

May 1997

Published Proceedings of the *11th Les Rencontres de Physique de la Vallée D'Aosta: Results and Perspectives in Particle Physics*, La Thuille, Italy, March 2-8, 1997

## **Disclaimer**

*This report was prepared as an account of work sponsored by an agency of the United States Government. Neither the United States Government nor any agency thereof, nor any of their employees, makes any warranty, expressed or implied, or assumes any legal liability or responsibility for the accuracy, completeness, or usefulness of any information, apparatus, product, or process disclosed, or represents that its use would not infringe privately owned rights. Reference herein to any specific commercial product, process, or service by trade name, trademark, manufacturer, or otherwise, does not necessarily constitute or imply its endorsement, recommendation, or favoring by the United States Government or any agency thereof. The views and opinions of authors expressed herein do not necessarily state or reflect those of the United States Government or any agency thereof.*

## **Distribution**

*Approved for public release; further dissemination unlimited.*

CDF/4176
----------

RU 97/E-31
------------

## JET PHYSICS AT CDF\*

Philip Mèlèse

*The Rockefeller University*

(Representing the CDF collaboration)

### Abstract

We present high  $E_T$  jet measurements from CDF at the Fermilab Tevatron Collider. The inclusive jet cross section at  $\sqrt{s} = 1800$  GeV with  $\sim 5$  times more data is compared to the published CDF results, preliminary D0 results, and next-to-leading order QCD predictions. The  $\sum E_T$  cross section is also compared to QCD predictions and the dijet angular distribution is used to place a limit on quark compositeness.

The inclusive jet cross section at  $\sqrt{s} = 630$  GeV is compared with that at 1800 GeV to test the QCD predictions for the scaling of jet cross sections with  $\sqrt{s}$ . Finally, we present momentum distributions of charged particles in jets and compare them to Modified Leading Log Approximation predictions.

---

\*Presented at Les Rencontres De Physique De La Vallée D'Aoste, La Thuile, March 1997

# 1 Introduction

The jet data from the Tevatron can be used to test perturbative QCD where next-to-leading order (NLO) QCD calculations[1] should produce accurate predictions. The highest  $E_T$  jets also provide a sensitive probe of quark substructure down to  $O(10^{-17})$  cm. Although the published CDF inclusive jet cross section[2] is remarkably well described by the NLO QCD prediction for jets with  $E_T$  between 15 and 400 GeV, the data are systematically above the prediction for  $E_T > 200$  GeV. This has stimulated both the experimentalist to verify the data and the theorist to investigate the limitations of the predictions.

A potentially more serious problem for QCD comes from testing the  $\sqrt{s}$  scaling of the jet cross sections. The naive parton model predicts that the jet cross section should scale as  $x_T = 2E_T/\sqrt{s}$ , and the formal NLO QCD prediction has been calculated. An earlier comparison between  $\sqrt{s} = 546$  and 1800 GeV jets[3] found a disagreement between the data and NLO QCD predictions at low values of  $x_T$ . This comparison has been redone with the more recent  $\sqrt{s} = 630$  and 1800 GeV jet data.

## 2 Jet Identification and Data Sample

The CDF detector has been described in detail elsewhere[4]. The elements of the detector which are used in these jet measurements are the central electromagnetic and hadronic calorimeters. The calorimeters are segmented in pseudo-rapidity<sup>†</sup>  $\eta$  and azimuth  $\phi$  with a projective tower geometry. To balance the statistics in the different jet  $E_T$  bins, the data were collected with different jet  $E_T$  triggers using appropriate prescale factors. The analyzed data were taken during two Tevatron running periods: run 1A with  $\sim 20$  pb<sup>-1</sup> collected during 1992/93; and run 1B with  $\sim 90$  pb<sup>-1</sup> collected during 1994/95.

Jets were reconstructed using a cone algorithm[5] with radius  $R \equiv (\Delta\eta^2 + \Delta\phi^2) = 0.7$  and the QCD calculation uses a similar algorithm[1]. The jets are required to have  $0.1 < |\eta| < 0.7$  to be well measured within the central calorimetry. The energy from the fragmentation of partons not associated with the hard scattering (underlying event energy) is subtracted from the jet energy. No correction is applied for jet energy falling outside of the cone because this should be modeled by the NLO QCD calculations.

---

<sup>†</sup>The pseudo-rapidity is defined as  $\eta \equiv -\ln[\tan(\theta/2)]$ , where  $\theta$  is the polar angle with respect to the beam line.

### 3 Inclusive Jet Cross Section at 1800 GeV

The inclusive jet cross section is defined as

$$\frac{1}{\Delta\eta} \int d\eta \frac{d^2\sigma}{dE_T d\eta} = \frac{1}{\Delta\eta} \frac{1}{L} \frac{N_{jet}}{\Delta E_T},$$

where  $L$  is the integrated luminosity, and  $N_{jet}$  is the number of jets in a  $\Delta E_T$  bin. The effect of finite jet resolution on a steeply falling spectrum was corrected using an unsmearing procedure[2]. The jet resolution is determined by combining the single particle response, from test beam data and isolated tracks in the central tracking chamber, with the particle momentum distribution within jets provided by a tuned Field-Feynman fragmentation model. A hypothetical curve from the assumed underlying physics is convoluted with the jet resolution and the  $\chi^2$  is calculated between it and the measured spectrum. After adjusting the parameters of the physics curve to minimize the  $\chi^2$  difference, this curve represents our best guess at the underlying physics spectrum. The measured spectrum is then “unsmearred” in both  $E_T$  and cross section using the difference between the physics curve before and after jet resolution effects. The jet spectra, including the  $\sum E_T$ , in this report have all been corrected in this way.

The 1989 CDF inclusive jet cross section[6] was based on  $4.2 \text{ pb}^{-1}$  of data taken at  $\sqrt{s} = 1800 \text{ GeV}$ . The cross section was shown to be consistent with NLO QCD predictions for jets with  $E_T$  between 35 and 450 GeV with a possible excess over theory at the highest values of  $E_T$ . The more recent published result[2] is based on  $19.5 \text{ pb}^{-1}$  (run 1A) and the measured spectrum is shown in Fig.1 (left plot). The measured inclusive jet rate for  $E_T > 200 \text{ GeV}$  is systematically above the NLO QCD prediction using the MRSD0' parton distribution function (PDF). The probability that the excess above  $E_T = 200 \text{ GeV}$  is consistent with this QCD prediction has been calculated to be 1% taking into account the statistical and correlated systematic uncertainties. Other PDFs reduce the significance of the excess, but cause disagreement at lower  $E_T$ .

### 4 Verification of measured Jet Cross Section

To verify this experimental result, CDF has remeasured the inclusive jet cross section using  $87 \text{ pb}^{-1}$  of data from run 1B. Figure 1 (right plot) shows that the 1A and 1B cross sections are consistent with each other and they both show a systematic excess at high  $E_T$  compared to a NLO QCD prediction using CTEQ3M, a more modern PDF than

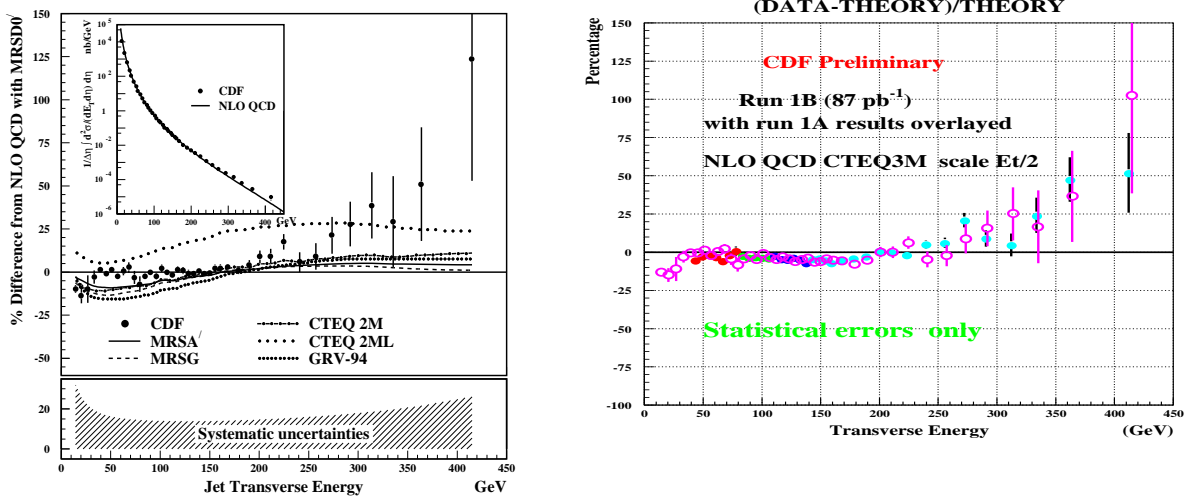


Figure 1: **Left Plot:** The percent difference between the CDF inclusive jet cross section at  $\sqrt{s} = 1800$  GeV and the NLO QCD prediction. The error bars represent statistical errors, while the quadratic sum of the correlated systematic errors are shown by the hatched region at the bottom. The effect of different PDFs are shown relative to MRSD0'. The measured and predicted spectra are compared on a log scale in the inset. **Right Plot:** The percent difference between the measured 1A (open circles) and 1B (closed circles) cross sections and the NLO QCD prediction using the CTEQ3M PDF.

MRSD0' which was used in the run 1A prediction. The 1B cross section presented here is preliminary, with statistical errors only.

The D0 collaboration also has a preliminary inclusive jet cross section at  $\sqrt{s} = 1800$  GeV based on  $93 \text{ pb}^{-1}$  of data (run 1A and 1B). The D0 and CDF (run 1B) data are shown together in Fig. 2 (left) compared to NLO QCD predictions using two new PDFs described in section 5 below. From these plots it is clear that the CDF and D0 data are consistent with each other after adjusting their relative normalization within the systematic uncertainties. An improved D0 inclusive jet cross section, including systematic errors, was shown at this conference[7]. The CDF and D0 data are still statistically consistent within normalization uncertainties. One outstanding issue in the comparison of the D0 and CDF results is the implementation of the NLO QCD calculations and PDFs.

An alternative test of QCD using jets is to measure the cross section as a function of  $\sum E_T$ , the sum over all jet  $E_T$  in an event (no  $\eta$  requirement). The unsmeared  $\sum E_T$  cross section, using  $E_T > 100$  GeV jets, is shown in Fig. 2 (right plot) divided by NLO QCD predictions using several PDFs. The high  $\sum E_T$  data are also above the predictions, but the large systematic uncertainties reduce the significance of the effect.

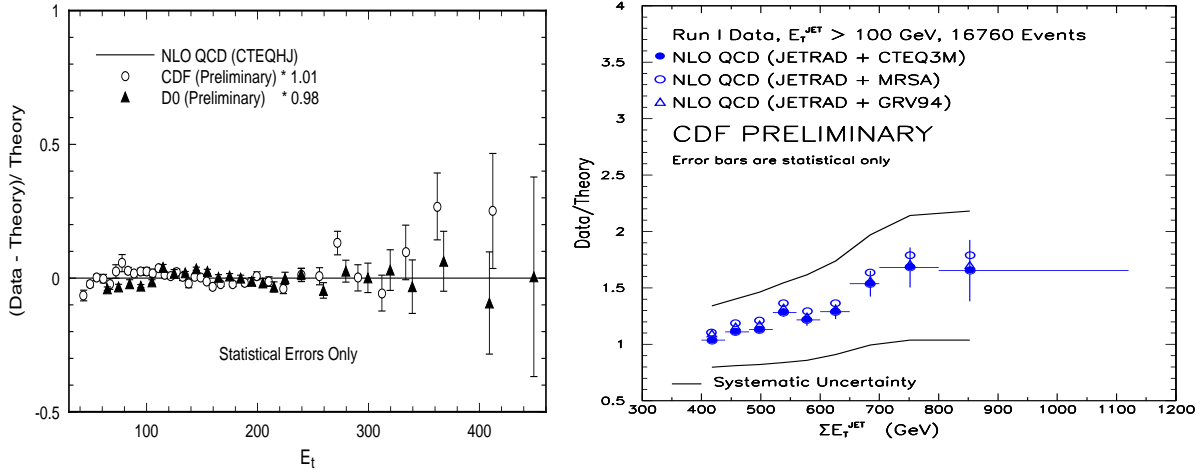


Figure 2: **Left Plot:** The percent difference between inclusive jet data, both CDF and D0, and a NLO QCD prediction using a new PDF, CTEQHJ, which includes the CDF jet data with increased weight at high  $E_T$ . **Right Plot:** The  $\Sigma E_T$  spectrum divided by the NLO QCD prediction using different PDFs.

## 5 Interpretation of High $E_T$ Jet Results

The excess at high  $E_T$  seen in the inclusive jet data has stimulated a great deal of theoretical activity. The CTEQ collaboration has derived new PDFs which include the CDF and D0 jet data[8]. The high  $E_T$  CDF jet data has an insignificant contribution to the global fit (CTEQ4M) because of their large errors. There is another PDF, CTEQHJ, which gives additional weight to the high  $E_T$  jet data, while maintaining agreement with the other data used in the PDF fit. In this case the CDF high  $E_T$  data has been made consistent with this QCD prediction, as seen in Fig. 2 (left plot). Therefore the CDF data can be explained by modifying the PDFs without violating other experimental results. This is because the gluon distribution isn't well constrained in the regime responsible for high  $E_T$  jet production.

There have also been studies of QCD corrections to the inclusive jet predictions. For example, the effects of soft gluon resummation[9] and the choice of factorization scheme[10], DIS or  $\overline{MS}$ , have been investigated. There were also some more exotic explanations for the high  $E_T$  jet excess, but the data at present is compatible with the standard model.

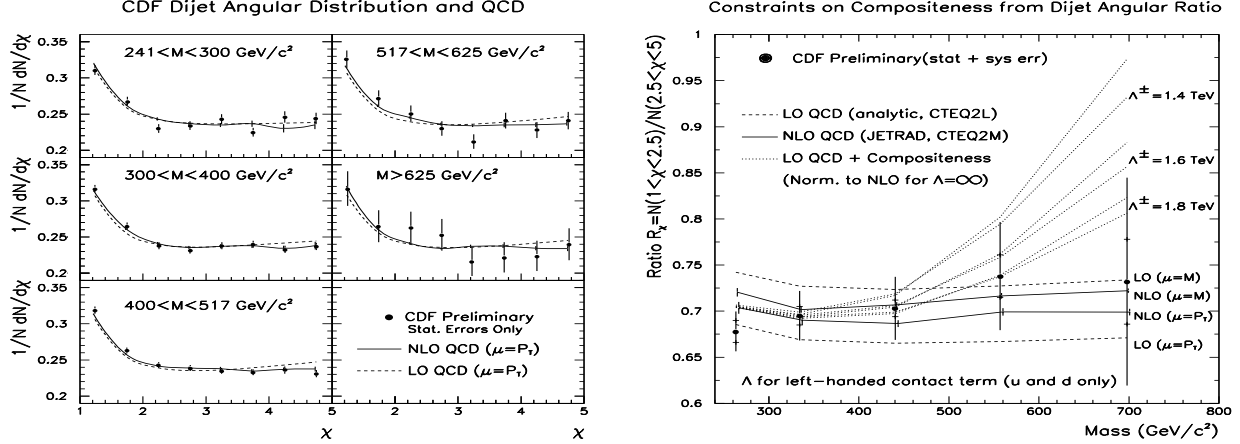


Figure 3: **Left Plot:** The angular distribution  $\chi = \exp |\eta_1 - \eta_2|$  is shown for various dijet masses compared to leading order and NLO QCD predictions. **Right Plot:** The  $\chi$  ratio  $R_\chi = N(\chi < 2.5)/N(\chi > 2.5)$  is shown versus dijet mass with statistical (inner error bars) and systematic errors (outer error bars). The distributions are compared to QCD predictions and 95% limits on the compositeness scale are shown.

## 6 Dijet Angular Distribution

The dijet angular distribution can be used to check for quark substructure, and is complementary to the inclusive jet spectrum. In lowest order the dijet production cross section factorizes into a PDF dependent term and another which depends on the center of mass scattering angle  $\theta^*$  with respect to the proton beam direction. The dijet angular distribution is typically expressed in terms of  $\chi$ :

$$\chi = \exp |\eta_1 - \eta_2| = \frac{(1 + |\cos \theta^*|)}{(1 - |\cos \theta^*|)}.$$

This variable flattens out the t-channel pole expected from QCD and makes it easier to observe a more isotropic contribution, from quark compositeness for instance. We calculate  $\chi$  using the two largest  $E_T$  jets above 15 GeV with  $|\eta| < 2.0$  and restrict  $\chi < 5$  ( $\cos \theta^* < 2/3$ ). Figure 3 (left plot) shows the measured  $\chi$  distributions using  $106 \text{ pb}^{-1}$  of data for different dijet mass bins compared to leading order and NLO QCD predictions.

An isotropic component due to quark substructure would be observed as a low- $\chi$  enhancement at high dijet masses. For this reason, we use a variable  $R_\chi$  which is sensitive to the difference between the low  $\chi$  and high  $\chi$  regions:

$$R_\chi = \frac{N(\chi < 2.5)}{N(\chi > 2.5)},$$

where  $N$  is the number of events in each region. Figure 3 (right plot) shows the measured  $R_\chi$  versus dijet mass compared to QCD predictions. The expected excess at high dijet mass is shown for a flavor-symmetric left-handed composite model with different contact interaction scales  $\Lambda$ . The data are in agreement with NLO QCD, which allows us to set a 95% confidence level limit on this particular contact interaction, assuming only  $u$  and  $d$  quarks are composite, of 1.8 TeV for positive interference ( $\Lambda^+$ ) and 1.6 TeV for negative interference ( $\Lambda^-$ ). These limits essentially rule out the compositeness interpretation of the high  $E_T$  excess in the inclusive jet cross section.

## 7 Inclusive Jets at 630 GeV and $x_T$ scaling

Another unsolved mystery for QCD is the scaling of the jet cross section with  $\sqrt{s}$ . The naive parton model predicts that the inclusive jet cross section should scale as  $x_T = 2E_T/\sqrt{s}$ . This scaling is violated in part due to the running of  $\alpha_s$  and the  $Q^2$  evolution of the PDFs, but the complete NLO QCD prediction is well determined. There is an earlier CDF published result[3] comparing 7.5 nb<sup>-1</sup> of data at  $\sqrt{s} = 546$  with 4.2 pb<sup>-1</sup> of  $\sqrt{s} = 1800$  GeV data. The ratio of the two inclusive jet cross sections versus  $x_T$  was found to disagree with QCD predictions below  $x_T \sim 0.15$ . In order to verify this result, 600 nb<sup>-1</sup> of jet data was collected at  $\sqrt{s} = 630$  GeV and analyzed.

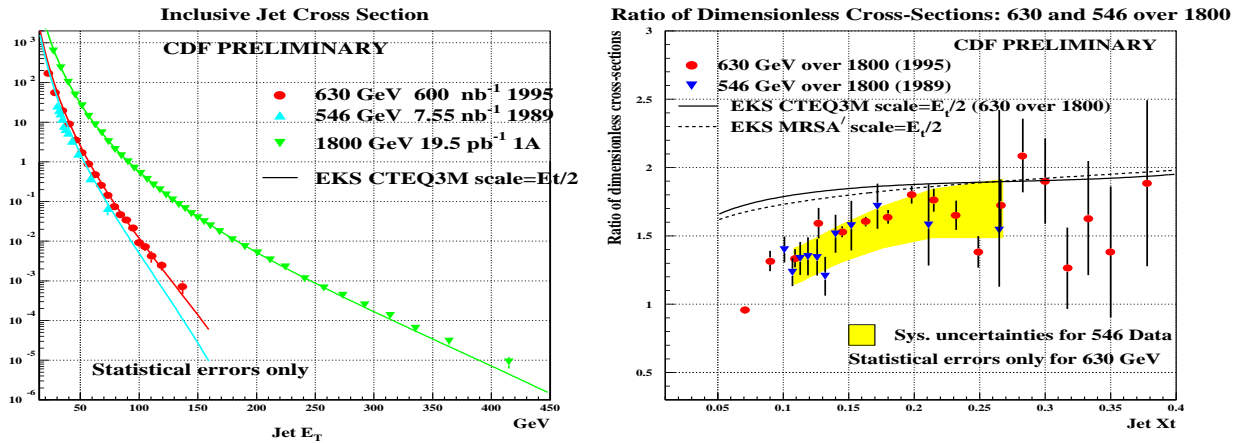


Figure 4: **Left Plot:** The inclusive jet cross sections for 1800, 630 and 546 GeV compared to a NLO QCD prediction. **Right Plot:** The ratio of 630/1800 and 546/1800 cross sections versus  $x_T = 2E_T/\sqrt{s}$  compared to NLO QCD predictions.

The inclusive jet cross section at  $\sqrt{s} = 630$  GeV was derived in the same way as the 1800 GeV results described above. Figure 4 (left plot) shows the inclusive jet cross sections versus  $E_T$  for  $\sqrt{s} = 546, 630$  and 1800 GeV, which agree very well with the NLO QCD predictions. Figure 4 (right plot) shows the ratio of cross sections, 546 over 1800 and 630 over 1800, versus  $x_T$ . Both ratios are consistent with each other but are significantly lower than the NLO QCD predictions at low values of  $x_T$ . The ratio of cross sections is relatively insensitive to the PDF choice and detector effects and normalization uncertainties tend to cancel. This is not a jet  $E_T$  effect because the  $\sqrt{s} = 630$  GeV cross section is  $\sim 20\%$  lower than NLO QCD predictions in the same region of jet  $E_T$  where the 1800 GeV data is in good agreement.

## 8 Jet Fragmentation and Scaling

The high  $E_T$  dijets were also used to test Modified Leading Log Approximation (MLLA) predictions for jet fragmentation. The fragmentation process may be separated into a short distance (high energy) perturbative regime and a long distance (low energy) non-perturbative hadronization regime. The boundary can be characterized by a  $k_T$  cut-off scale  $Q_0$ , where perturbative calculations in  $\alpha_s$  are valid for  $Q_0 \gg \Lambda_{QCD}$ . For instance the scale could be defined as where single gluon emission probability,  $\sim \alpha_s \ln^2(E_{jet}/Q_0)$ , becomes unity, which for  $E_{jet} = 200$  GeV is at  $Q_0 \sim 10$  GeV. A significant component of jets has  $p_T < 10$  GeV, so perturbative QCD based on  $\alpha_s$  expansion cannot be used to predict jet fragmentation.

The double log term in single gluon emission originates from soft ( $\sim dk/k$ ) and collinear ( $\sim dk_T/k_T$ ) divergencies. This problem is overcome in the Leading Log Approximation[11], where the dominant (leading log) contributions are summed to all orders in  $\alpha_s$ . The approximation was improved by incorporating angular ordering to account for color interference effects and then the next-to-leading log terms were calculated to provide the Modified Leading Log Approximation[12]. The MLLA can describe many intra-jet features with essentially no free parameters. The calculations are infrared stable down to  $Q_0 = \Lambda_{QCD}$ , where this limit will be left as a free parameter,  $Q_{eff}$ , in comparing the theory to data.

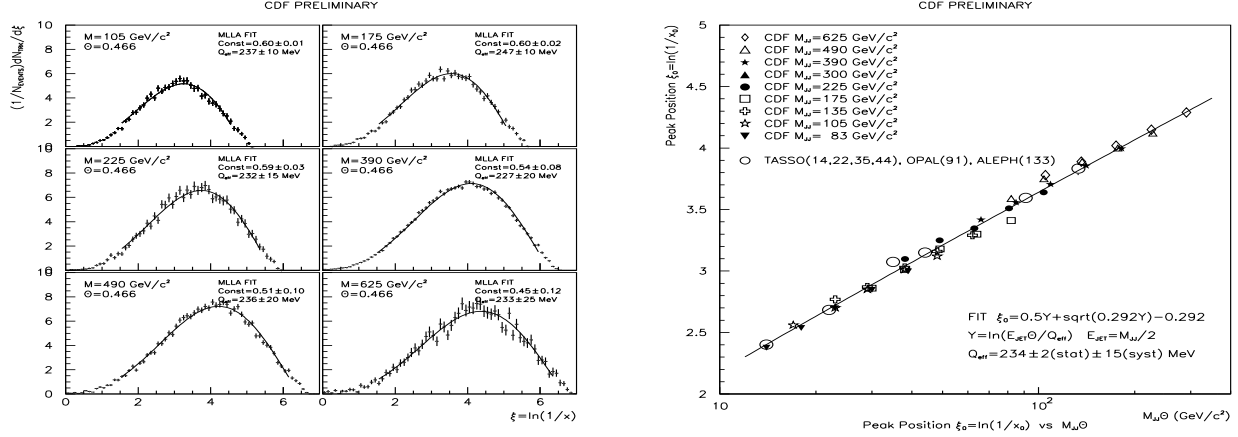


Figure 5: **Left Plot:** Momentum distributions of charged particles in jets, plotted as  $\xi = \ln 1/x$  where  $x = p_{trk}/E_{jet}$ , for tracks within a cone angle of  $\theta_{cone} = 0.446$  for different dijet masses ( $M_{JJ}$ ). The curves are fit to to the predicted MLLA distribution, with a normalization constant (Const) and cutoff scale  $Q_{eff}$  allowed to vary. **Right Plot:** The peak position,  $\xi_0$ , of the momentum distribution as a function of  $M_{JJ} \cdot \theta_{cone}$ . The data points are from CDF and  $e^+e^-$  experiments and are fit to the MLLA prediction with  $Q_{eff}$  as a free parameter.

The MLLA formula that describes the momentum distribution of particles within a jet for dijet events with mass  $M_{JJ}$  is:

$$\frac{1}{N_{events}} \frac{dN_{trk}}{d\xi} = Const \cdot f_{MLLA}(Y, \xi)$$

$$\xi \equiv \ln \frac{1}{x}; \quad x = \frac{p_{trk}}{E_{jet}}; \quad Y = \ln \frac{E_{jet} \cdot \theta_{cone}}{Q_{eff}}; \quad E_{jet} \equiv \frac{M_{JJ}}{2}$$

where  $p_{trk}$  is the momentum of a charged particle (track) within a cone of angle  $\theta_{cone}$  with respect to the jet axis. The function  $f_{MLLA}$  is the MLLA formula for the number of final state partons per unit  $\xi$  per event (dijet) for gluon jets. In order to fit the MLLA prediction to the measured track momentum distribution within jets, the constant ‘‘Const’’ takes into account the number of hadrons per parton (hadronization), the fraction of charged to all particles (2/3 if all pions), and the fraction of quark jets (quarks contribute 4/9 compared to gluons).

Figure 5 (left plot) shows the measured momentum distribution, plotted as  $\xi = \ln(E_{jet}/p_{trk})$ , for tracks within  $\theta_{cone} = 0.466$  of the jet axis for dijet masses between 105 and 625 GeV. The MLLA formula is fit within its region of validity:  $\xi > 1.6$  to insure

$x \ll 1$  and the upper  $\xi$  bound corresponds to  $p_T > Q_{eff}$ . The fitted values of  $Q_{eff}$  are consistent within errors and the decrease of “Const” with increasing dijet mass is expected from the increased fraction of quark jets. These plots show that the MLLA successfully describes the momentum distribution of charged particles within high  $E_T$  jets.

Another MLLA prediction is that the position  $\xi_0$  of the peak of the momentum distribution depends only on  $Y$ :  $\xi_0 = \frac{1}{2}Y + \sqrt{cY} - c$ , where  $c=0.29$  ( $0.32$ ) for 3 (5) quark flavors. Figure 5 (right plot) shows the peak position  $\xi_0$  versus  $M_{JJ}\theta_{cone}$  on a log scale, which is related to  $Y = \ln(E_{jet} \cdot \theta_{cone}/Q_{eff})$ , for these CDF data and  $e^+e^-$  experiments. The MLLA formula fits well assuming 3 flavors ( $c=0.29$ ) and we can extract  $Q_{eff} = 234 \pm 2$  (stat)  $\pm 15$  (syst) MeV.

## 9 Conclusions

The CDF jet data have produced many interesting results. The excess of high  $E_T$  jets over QCD predictions in the inclusive jet spectrum at  $\sqrt{s} = 1800$  has persisted after analyzing more data (run 1B) and also appears in the  $\sum E_T$  spectrum. The D0 inclusive jet spectrum is consistent with CDF within normalization uncertainties. However, there are discrepancies in the way D0 and CDF compare to the NLO QCD predictions.

The excess can be explained by modifying the gluon distribution in the proton, which is not well constrained by experiments contributing to the current PDFs. The compositeness interpretation of the high  $E_T$  jet excess is essentially ruled out by the limits on the contact term coming from the CDF dijet angular distributions.

There is an even more interesting discrepancy between QCD and jet data when comparing jet cross sections at different  $\sqrt{s}$ . The ratio of 630 over 1800 GeV jet cross sections, versus the scaling variable  $x_T = 2E_T/\sqrt{s}$ , is significantly below QCD predictions for  $x_T < 0.15$ . This verifies the previous CDF result comparing 546 to 1800 GeV jet cross sections. In this case both the uncertainty on the QCD prediction, due to PDF or choice of renormalization scale, and the data, due to detector effects, tend to cancel in the ratio of cross sections.

Finally, the MLLA predictions for the momentum distribution of particles within jets are remarkably successful in describing the CDF data. This tests the domain of QCD predictions down to  $\Lambda_{QCD} \sim Q_{eff} = 234 \pm 2$  (stat)  $\pm 15$  (syst) MeV.

## References

- [1] S. Ellis *et al.*, Phys. Rev. Lett. **64**, 2121 (1990);  
F. Aversa *et al.*, Phys Rev. Lett. **65**, 401 (1990);  
W.T. Giele *et al.*, Nucl. Phys. **B403**, 633 (1993).
- [2] F. Abe *et al.* (CDF Collaboration), Phys. Rev. Lett. **77**, 438 (1996).
- [3] F. Abe *et al.* (CDF Collaboration), Phys. Rev. Lett. **70**, 1376 (1993).
- [4] F. Abe *et al.* (CDF Collaboration), Nucl. Instrum. Methods **A271**, 387 (1988).
- [5] F. Abe *et al.* (CDF Collaboration), Phys. Rev. **D45**, 1448 (1992).
- [6] F. Abe *et al.* (CDF Collaboration), Phys. Rev. Lett. **68**, 1105 (1992).
- [7] see the talk on “Jet Production at D0” given by V. D. Elvira at this conference.
- [8] H.L. Lai and W.K. Tung, hep-ph/9605269 (1996).
- [9] S. Catani *et al.*, hep-ph/9604351 (1996).
- [10] M. Klasen and G. Kramer, hep-ph/9605210 (1996).
- [11] See review by A. Basseto, M. Ciafanoli and G. Marchesini, Phys. Rep. **C100**, 201 (1983).
- [12] A.H. Mueller, Nucl. Phys. **B213**, 85 (1983), erratum in **B241**, 141 (1984);  
Y. Dokshitzer and S. Troyan, XIX Winter School of LNPI, Vol. 1, p. 144, Leningrad;  
E.D. Malaza and B.R. Webber, Phys. Lett. **B149**, 501 (1984).